

## THE ORBITAL LIGHT CURVE OF PSR 1957+20

PAUL J. CALLANAN

Center for Astrophysics, 60 Garden Street, Cambridge, MA 02138

AND

JAN VAN PARADIJS<sup>1</sup> AND ROELAND RENGELINK

Astronomical Institute “Anton Pannekoek,” University of Amsterdam, Kruislaan 403, 1098 SJ Amsterdam, The Netherlands;  
 and Center for High Energy Astrophysics, NIKHEF-H

Received 1994 May 19; accepted 1994 August 3

### ABSTRACT

We make a detailed study of the optical light curve of PSR 1957+20. We show that the deep, smooth, and symmetrical modulation can be successfully modeled by a highly irradiated secondary. Two types of models are consistent with the data: (1) a secondary close to filling its Roche lobe with 10%–20% of the incident flux converted to optical emission, and (2) a secondary considerably underfilling its Roche lobe, with a high degree of beaming of the neutron star flux. However, the second model can be rejected on the basis of current estimates of the extinction toward 1957+20. The proximity of the photosphere of the secondary to its Roche lobe facilitates mass loss by irradiation. Our ignorance of the (nonirradiated) luminosity of the secondary allows us to place only weak constraints on the inclination—50°–80°. There is no evidence in the light curve for optical emission from any source in PSR 1957+20 other than the secondary itself.

*Subject headings:* binaries: close — pulsars: individual (PSR 1957+20) — stars: neutron

### 1. INTRODUCTION

Binary millisecond pulsars are most easily explained as the progeny of low-mass X-ray binaries (LMXBs). Once the envelope of the mass donor is exhausted and accretion onto the neutron star finally ceases, the neutron star “turns on” as a radio pulsar. The angular momentum accreted during the LMXB phase results in a rapidly spinning neutron star (with spin period  $\sim 1$ –100 ms), in contrast to the much longer spin periods expected of an old, isolated radio pulsar (see Bhattacharya & van den Heuvel 1991 for a discussion of the various evolution scenarios). However, the discovery of old, isolated millisecond pulsars is more difficult to understand.

PSR 1957+20 occupies a unique place in our understanding of the evolution of binary to isolated millisecond pulsars (Fruchter, Stinebring, & Taylor 1988). It is the only known binary for which the effect of irradiation by the radio pulsar on the secondary has been directly observed: the optical counterpart varies by  $\geq 3$  mag in  $R$  throughout the 9.17 h orbital cycle (Fruchter et al. 1988; van Paradijs et al. 1988). At radio wavelengths, emission from the pulsar is eclipsed for  $\sim 10\%$  of the orbital cycle: the eclipsing region is much larger than even the Roche lobe of the secondary, implying that a wind of material is being driven from the secondary by irradiation from the neutron star. It has been suggested that the flux from the neutron star will eventually evaporate the secondary entirely, leaving an isolated millisecond pulsar (e.g., van den Heuvel & van Paradijs 1988), but the timescale of this evaporation and the details of the evaporation process are currently subject to debate (e.g., Eichler & Levinson 1988). Two similar systems have subsequently been discovered—the globular cluster binary millisecond pulsars in Terzan 5 (Lyne et al. 1990) and NGC 6342 (Lyne et al. 1993); however, for these two systems no optical identifications have yet been made. Hence

PSR 1957+20 is by far the best studied of these systems en route to “widowhood.”

Efforts to understand the detailed physics of this evaporation mechanism have been hampered by the considerable uncertainties which still exist in many of the basic parameters of this system. Initial estimates of the distance to the pulsar, and the temperature of the companion at maximum, lead observers to conclude that the companion underfilled its Roche lobe by a factor of  $\sim 2$  and was probably degenerate (e.g., Fruchter et al. 1988). However, the distance to PSR 1957+20 has recently been revised upward to 1.6 kpc (with an uncertainty of 50%)—the increased absolute magnitude now implies that the secondary fills its Roche lobe, facilitating the evaporation process (Fruchter & Goss 1991). An asymmetry in the optical light curve reported by Djorgovsky & Evans (1988), interpreted as due to the shock at the interface between the winds from the neutron star and secondary (see also Eichler 1991), was not observed by Callanan, Charles, & van Paradijs (1991). Only marginal evidence was presented in the latter paper for the color change expected of such a large heating effect.

Optical observations are severely complicated by the presence of a line-of-sight contaminator only 0'.8 from the counterpart of the pulsar. This star is of comparable magnitude to PSR 1957+20 at maximum, and resolving it from the pulsar requires exceptional observing conditions. In an effort to better determine the light curve, and constrain the parameters of PSR 1957+20 (e.g., the orbital inclination, the flux incident on the secondary, the fraction of Roche lobe filled by the secondary) we obtained four nights of photometry using the 4.2 m William Herschel Telescope (WHT) on La Palma.

### 2. OBSERVATIONS

We observed PSR 1957+20 with the WHT on the nights of 1989 July 2–5 with a GEC (P8603) chip at the Cassegrain focus of the telescope. Using Taurus-2 as a focal reducer we obtained

<sup>1</sup> Also Physics Department, University of Alabama, Huntsville.

a plate scale of  $0''.27 \text{ pixel}^{-1}$ . We cycled through  $B$ ,  $V$ , and  $R$  (Johnson) filters near maximum light, and through  $V$  and  $R$  only through minimum. For the nights of July 2 and 5,  $\sim 0''.8$  seeing and especially stable atmospheric conditions allowed us to resolve the pulsar from its contaminator: for the other two nights the seeing was such that this task was made much more difficult.

The data were debiased and flat-fielded, and the IRAF implementation of DAOPHOT (Stetson 1987) was used to (1) deconvolve the image of the pulsar from the contaminator, and (2) perform photometry of the pulsar relative to a series of nearby stars. For those frames where the pulsar and its contaminator could not be resolved, we proceeded as follows. We first obtained the positions of the pulsar, its contaminator, and a series of 10 bright comparison stars from images taken under good seeing conditions ( $\leq 0''.8$ ). The positions of these bright stars were then measured in each of the poorer quality frames and used to determine the expected position of the pulsar and its contaminator in each frame. Finally, the relative magnitudes of these stars were determined while keeping these positions fixed. Although this greatly improves the quality of the resulting light curves, this technique is extremely sensitive to small errors in the determined positions of the pulsar and the contaminator. The resulting light curves were then calibrated using two Landolt (1983) standard stars. The  $B$ -,  $V$ -, and  $R$ -band magnitudes of PSR 1957+20 at maximum were found to be 21.08, 20.16, and 19.53 respectively ( $\pm 0.05$ ).

Simulations showed that the errors estimated by DAOPHOT, for stars of magnitude comparable to that of PSR 1957+20 near eclipse, were underestimated by  $\sim 50\%$ . The error bars for these data points ( $\pm 0.2$  in phase about eclipse) were increased accordingly. In order to estimate how far the results of the photometric analysis of this difficult object depend on the choice of the image-processing software, we made an independent analysis of the data with MIDAS. The results of the MIDAS and IRAF analyses are in very good agreement.

In Figure 1 (*upper panel*) we show the total  $R$ -band light curve of PSR 1957+20. For comparison, we plot in the lower panel the light curve of the contaminator star. In Figure 2 we present the  $R$ -band light curve of the pulsar obtained on the nights of July 2 and 5 (during which times DAOPHOT could easily deconvolve the contaminator), folded on the radio ephemeris of Ryba & Taylor (1992). Superimposed is the best-fit model discussed in § 3.

The modulation is smooth and symmetrical (as evidenced by the fitted model; see below), and is at least 4 mag deep (in  $R$ ). In Figure 3 we show the  $V - R$  data, again folded on the radio ephemeris. The color of the companion undergoes clear variability, as expected. We do not detect the companion at minimum, to a limiting magnitude of  $\sim 24$  in  $R$ .

### 3. DISCUSSION

The “fixed position” technique required to deconvolve the contaminator from the pulsar on the nights of July 3 and 4 introduces systematic errors which make a detailed comparison of these light curves difficult. However, it is apparent from the data obtained under the excellent seeing conditions of July 2 and 5 that the pulsar exhibits negligible intrinsic short-term variability either within an orbital cycle, or from one to another, to within our errors of measurement (see Fig. 2). This is in stark contrast to most other interacting binary systems (e.g., cataclysmic variables and X-ray binaries), where such variability is ubiquitous. This is consistent with the scenario of simple irradiation of the secondary by the spindown luminosity of the pulsar. The stability of the light curve provided us with a strong motivation to model our highest quality data in detail.

#### 3.1. The Model

The data were fitted to a simple model of an irradiated secondary, which has been used previously to analyze the orbital light curves of X-ray binaries (Tjemkes, van Paradijs, &

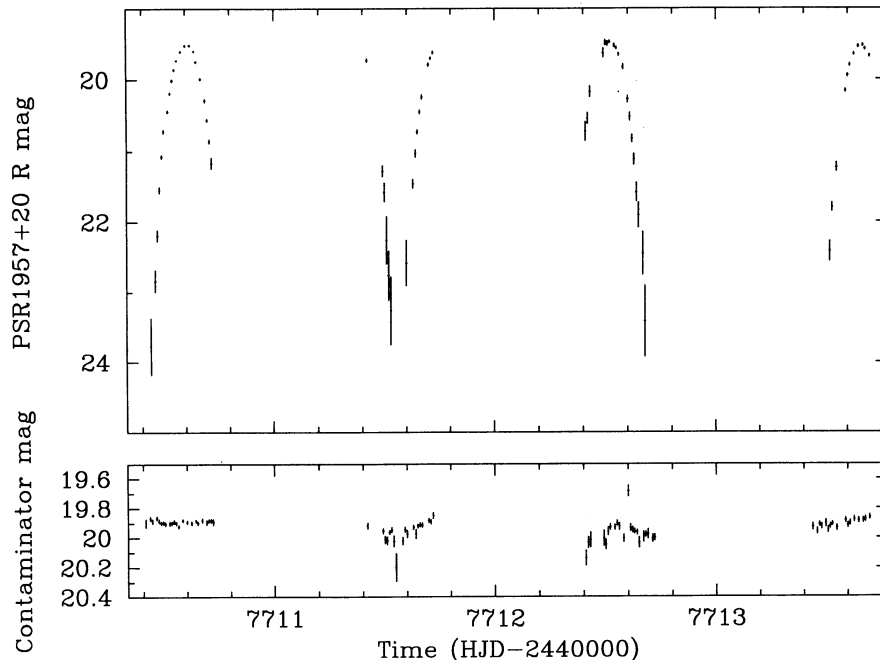


FIG. 1.— $R$ -band light curve of PSR 1957+20 and its contaminator

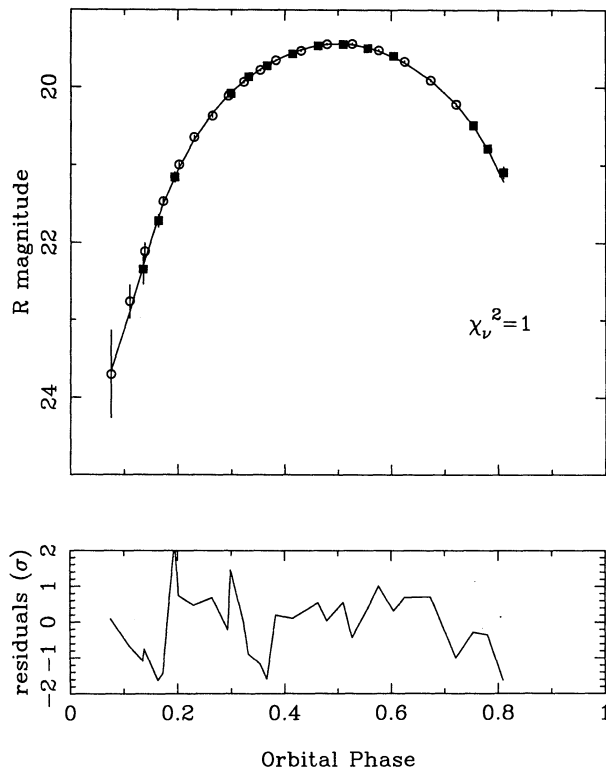


FIG. 2.—*R*-band light curve of PSR 1957+20 obtained during 1989 July 2 (squares) and 5 (circles), folded on the radio ephemeris. The data have been shifted by 0.25 in phase for consistency with standard nomenclature. The best-fit model ( $\eta = 20\%$ ,  $L_{\text{sec}} = 6 \times 10^{-3} L_{\odot}$ ,  $i = 75^{\circ}$ ,  $R_{\text{lobe}} = 0.9$ ) has been superimposed.

Zuiderwijk 1986; Heemskerk & van Paradijs 1990; refer to these papers for detailed descriptions of the program). We first fitted the *R* and *V* – *R* data from the July 2 observation and then checked for consistency with the entire data set. Four parameters were varied during the modeling, and the grid of values searched was as follows:

1. The fraction of its Roche lobe filled by the secondary ( $R_{\text{sec}}$ ):  $0.5 < R_{\text{sec}} < 1.0$ ;

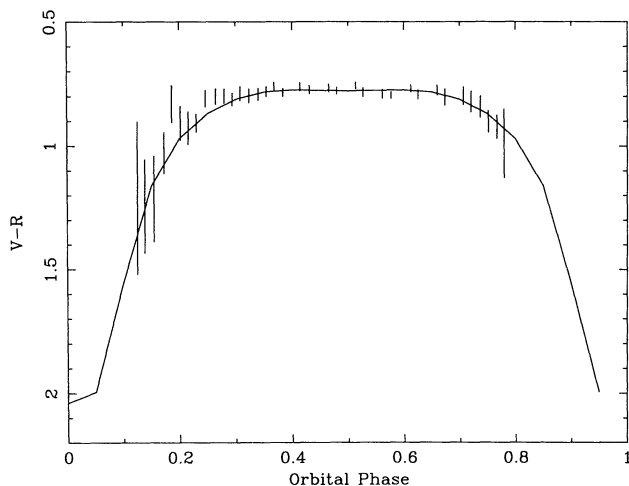


FIG. 3.—*V* – *R* variation of PSR 1957+20, with the same model superimposed.

2. The intrinsic (un-illuminated) luminosity of the secondary ( $L_{\text{sec}}$ ):  $2.5 \times 10^{-5} L_{\odot} < L_{\text{sec}} < 7.5 \times 10^{-3} L_{\odot}$ ;
3. The orbital inclination of the binary ( $i$ ):  $45^{\circ} < i < 90^{\circ}$ ;
4. The fraction of the energy flux from the neutron star (deriving from its spindown luminosity of  $1.5 \times 10^{35}$  ergs  $\text{s}^{-1}$ ) incident on the secondary surface that is converted into optical emission ( $\eta$ ):  $0.1 < \eta < 5.0$ .

The maximum value of  $L_{\text{sec}}$  was determined by the amplitude of the optical variability (for  $R_{\text{sec}} = 1$  and  $i = 90^{\circ}$ ). Values of  $\eta > 1$  were used to simulate the effect of beamed emission from the neutron star.

For each angle of inclination, the mass of the secondary and the size of its Roche lobe were recomputed using the radio pulsar timing data of Fruchter et al. (1988). The gravitational darkening was assumed to be that appropriate to late-type stars ( $F_{\nu} \propto g^{0.08}$ ; Lucy 1967), and the limb-darkening corrections used were the linearized approximations derived by Al-Naimiy (1978), which were extrapolated where necessary. For a given temperature, the fluxes at wavelengths corresponding to the *V* and *R* bands were estimated by interpolating a grid of stellar atmospheres; simple blackbody approximations are especially unrealistic for low ( $\leq 3000$  K) effective temperatures, where molecular line opacities begin to dominate the radiated flux. These fluxes were integrated across the passbands of our filters (i.e., standard Johnson). Differences between the flux of a blackbody and a stellar atmosphere at these low temperatures can easily exceed 1 mag in the *R* band. Hence, for temperatures greater than 3500 K, the flux was determined from an interpolation of a grid of Kurucz atmospheres (Kurucz 1993); for temperatures less than this, we used a grid of low-temperature atmospheres developed by Allard (1990). The latter have already been used to establish an effective temperature scale for the lower main sequence by Kirkpatrick et al. (1993; see also Allard et al. 1994). The minimum value of  $L_{\text{sec}}$  used during our parameter search was determined by the lowest temperature stellar atmosphere available (2000 K).

### 3.2. The Results

We find that the best-fit models (with  $\chi_{\nu}^2 = 1.2$  or better) fall into two categories: (1) relatively low values of  $\eta$  ( $\sim 7\%$ – $20\%$ ) and high values of  $R_{\text{sec}}$  ( $\sim 1.0$ ) and (2) high values of  $\eta$  ( $\geq 3$ ) and low values of  $R_{\text{sec}}$  ( $\sim 0.5$ ). The case 1 fits imply that the secondary is close to, but not quite filling, its Roche lobe: models with a lobe-filling secondary are inconsistent with our data. The case 2 fits are formally better than the case 1 fits, although the latter are statistically acceptable also (i.e.,  $\chi_{\nu}^2 = 0.8$  and 1.1, respectively). We show in Figures 4a and 4b the  $\chi^2$  contours for  $\eta$  and  $i$  for case 1 and 2 fits, respectively (for  $L_{\text{sec}} = 6.4 \times 10^{-3} L_{\odot}$ ).

### 3.3. The Efficiency

The case 2 fits imply a high degree of beaming. This would be consistent with the result of Manchester & Taylor (1977, p. 10), who found that the emission from only one out of every five pulsars is beamed toward the Earth; however, subsequent work has shown that for the fastest spinning pulsars, the radio emission is much more isotropic, and this ratio approaches unity (e.g., Narayan & Ostriker 1989). We believe we can exclude a high degree of beaming in the case of PSR 1957+20: values of  $\eta > 3$  imply effective temperatures across the secondary surface corresponding to an absolute *R* magnitude ( $M_R$ )

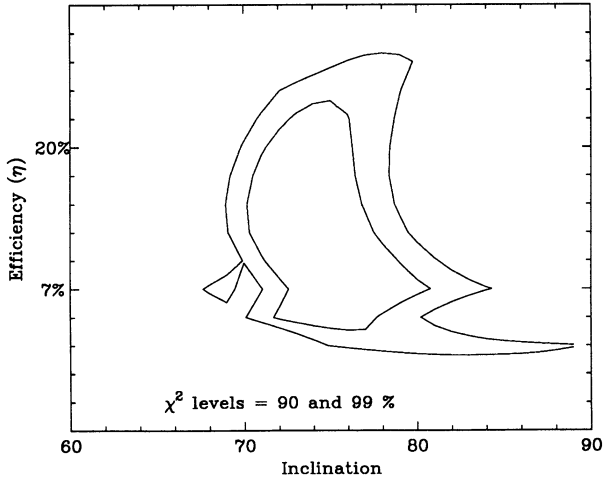


FIG. 4a

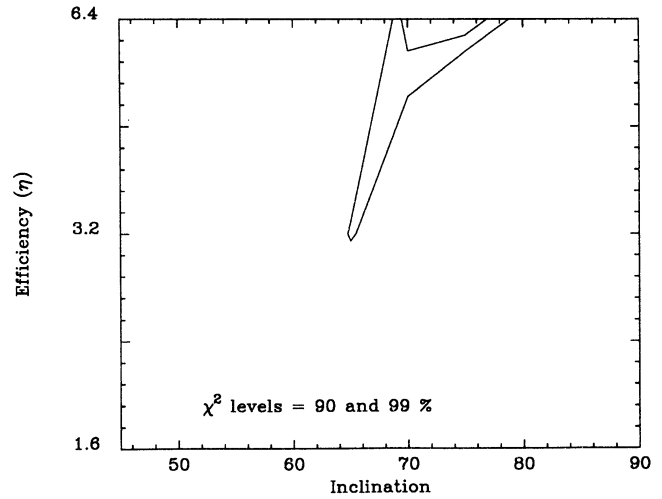


FIG. 4b

FIG. 4.— $\chi^2$  contour plots for case 1 (a) and case 2 (b) fits to the data ( $R_{\text{sec}} = 0.9$  and  $0.5$ , respectively). The intrinsic luminosity of the secondary ( $L_{\text{sec}}$ ) in each case is  $6.4 \times 10^{-3} L_{\odot}$ .

$\sim 6$ . For a distance of 1.6 kpc (Fruchter & Goss 1991), this would require an R-band extinction of  $\sim 2.5$  mag (corresponding to  $A_V \sim 3.5$  mag). Such a large visual extinction is inconsistent with the estimate of  $A_V < 1.0$  by Aldcroft, Romani, & Cordes (1992), made on the basis of optical spectroscopy of the bow-shock nebula around PSR 1957+20. Hence we will only consider the case 1 fits (low  $\eta$ , large  $R_{\text{sec}}$ ) for the rest of the discussion. In Figures 2 and 3 we have superimposed the light curve and color variation predicted by the model (for a case 1 fit and  $L_{\text{sec}} = 6.4 \times 10^{-3} L_{\odot}$ ).

### 3.4. The Distance

For a given  $\eta$  the temperature distribution on the secondary is determined, as is the expected color at maximum light. Then  $A_V$  is determined from the observed value of  $V-R$  at maximum. The quantity  $\eta$  also determines  $M_R$  (again at maximum), and hence the distance ( $D$ ) to the pulsar can also be

constrained. These estimates are essentially independent of  $L_{\text{sec}}$  (because of the degree of heating at maximum) and  $i$  (because of the increase in size of the Roche lobe with decrease in inclination). Taking  $E_{V-R} = 0.26 A_V$  (Allen 1973), we find that the observed  $V-R$  color of  $0.7 \pm 0.1$  implies  $10\% < \eta < 20\%$ . Corresponding values of  $A_V$  are  $0 < A_V < 0.8$ . The absolute R-band magnitude predicted by the models for these efficiencies then yield a distance range of  $1.6 < D < 3$  kpc. This distance estimate is consistent with that of Fruchter & Goss (1991).

### 3.5. The Inclination

Our limits on the orbital inclination ( $i$ ) are strongly dependent on the assumed value of  $L_{\text{sec}}$ . Decreasing  $L_{\text{sec}}$  lowers the minimum acceptable inclination. For  $L_{\text{sec}} = 6.4 \times 10^{-3} L_{\odot}$  (the maximum allowed for an acceptable  $\chi^2$ ),  $i = 75^\circ \pm 5^\circ$  (90% confidence; see Fig. 4a). Acceptable fits are also obtained for  $L_{\text{sec}} = 0$ :  $i = 55^\circ \pm 5^\circ$  (see Fig. 5). A detection of PSR 1957+20 in eclipse will reduce this large uncertainty on the inclination angle.

## 4. CONCLUSIONS

A detailed study of the optical light curve of PSR 1957+20 shows that the deep, smooth, and symmetrical modulation can be successfully modeled by a highly irradiated secondary. Two types of models are consistent with the data: (1) a secondary close to filling its Roche lobe with 7%–20% of the incident flux converted to optical emission, and (2) a secondary considerably underfilling its Roche lobe, with a high degree of beaming of the neutron star flux. However, the latter model is inconsistent with present estimates of the extinction toward 1957+20, implying that the secondary nearly fills its Roche lobe. This may greatly facilitate irradiation-induced mass loss. The inclination of the binary can only be constrained to be  $50^\circ$ – $80^\circ$ . There is no evidence for optical emission from any source in the system other than the secondary itself.

The Isaac Newton Group of telescopes is operated on the island of La Palma by the Royal Greenwich Observatory in the Spanish Observatorio del Roque de los Muchachos of the

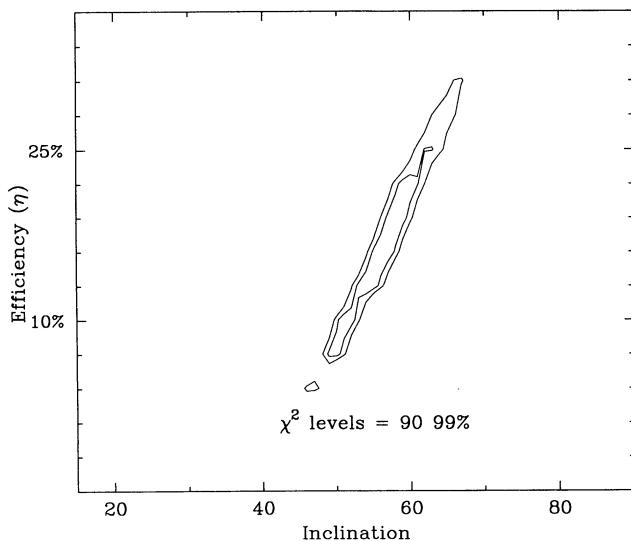


FIG. 5.—Same as Fig. 4 (with  $R_{\text{sec}} = 0.9$ ), but for  $L_{\text{sec}} = 0.0$ . This estimate of the inclination is the lower bound.

Instituto de Astrofísica de Canarias. We thank Martin Heemskerck for providing us with the original version of the light-curve modeling code and France Allard and Bob Kurucz for

making their atmospheres available to us. P. J. C. is supported by NASA through grant HF-1003.01-90A awarded by the Space Telescope Science Institute.

## REFERENCES

- Aldcroft, T. L., Romani, R. W., & Cordes, J. M. 1992, *ApJ*, 400, 638  
 Allard, F. 1990, Ph.D. thesis, Univ. Montréal  
 Allard, F., Hauschildt, P. H., Miller, S., & Tennyson, J. 1994, *ApJ*, 426, L39  
 Allen, C. W. 1973, *Astrophysical Quantities* (London: Athlone)  
 Al-Naimiy, H. M. 1978, *Ap&SS*, 53, 181  
 Bhattacharaya, D., & van den Heuvel, E. P. J. 1991, *Phy. Rep.*, 203, 1  
 Callanan, P. J., Charles, P. A., & van Paradijs, J. 1989, *MNRAS*, 240, 31p  
 Djorgovski, S., & Evans, C. R. 1988, *ApJ*, 335, L61  
 Eichler D. 1991, *MNRAS*, 254, 11p  
 Eichler, D., & Levinson, A. 1988, *ApJ*, 335, L67  
 Fruchter, A. S., & Goss, W. M. 1991, *ApJ*, 384, L47  
 Fruchter, A. F., Gunn, J. E., Lauer, T. R., & Dressler, A. 1988, *Nature*, 334, 686  
 Fruchter, A. S., Stinebring, D. R., & Taylor, J. H. 1988, *Nature*, 333, 237  
 Heemskerck, M. M., & van Paradijs, J. 1989, *A&A*, 223, 154  
 Kirkpatrick, J. D., Kelly, D. M., Rieke, G. H., Liebert, J., Allard, F., & Wehrse, R. 1993, *ApJ*, 402, 643  
 Kurucz, R. 1993, private communication  
 Landolt, A. U. 1983, *AJ*, 88, 439  
 Lucy, L. B. 1967, *Z. Astrophys.*, 65, 89  
 Lyne, A. G., et al. 1990, *Nature*, 347, 650  
 Lyne, A. G., Biggs, J. D., Harrison, P. A., & Bailes, M. 1993, *Nature*, 361, 47  
 Manchester, R. N., & Taylor, J. H. 1977, *Pulsars* (San Francisco: Freeman)  
 Narayan, R., & Ostriker, J. P. 1990, *ApJ*, 352, 222  
 Ryba, M. F., & Taylor, J. H. 1992, *ApJ*, 380, 560  
 Stetson, P. B. 1987, *PASP*, 99, 443  
 Tjemkes, S. A., van Paradijs, J., & Zuiderwijk, E. J. 1986, *A&A*, 154, 77  
 van den Heuvel, E. P. J., & van Paradijs, J. 1988, *Nature*, 334, 227  
 van Paradijs, J., et al. 1988, *Nature*, 334, 684